

Electronic and thermoelectric properties of Fe₂VAI: The role of defects and disorder

Daniel I. Bilc and Philippe Ghosez

Physique Théorique des Matériaux, Université de Liège (B5), B-4000 Liège, Belgium

Using first-principles calculations, we show that Fe₂VAI is an indirect band gap semiconductor. Our calculations reveal that its, sometimes assigned, semimetallic character is not an intrinsic property but originates from the antisite defects and site disorder, which introduce localized ingap and resonant states changing the electronic properties close to band gap. These states negatively affect the thermopower S and power factor $PF=S^2\sigma$, decreasing the good thermoelectric performance of intrinsic Fe₂VAI.

PACS numbers: 71.15.-m, 71.15.Mb, 71.20.-b, 71.20.Be, 71.20.Nr, 71.23.-k, 72.10.-d, 72.15.-v, 72.15.Jf

Energy-related issues are becoming more and more crucial. Devices based on thermoelectric (TE) materials are very appealing in this context, and they are one of the main thrusts in energy research on the global scale. They can be used for cooling or heating and for energy generation from recovered waste heat. The efficiency of a TE material depends on the dimensionless TE figure of merit, $ZT=(S^2\sigma T)/\kappa_{th}$, where σ is the electrical conductivity, S is the thermopower, T is the absolute temperature, and κ_{th} is total thermal conductivity which has electronic and lattice contributions. Improving the TE efficiency is not obvious because the different parameters entering ZT are linked and compete with each others. Moreover, ZT has to be maximized in the regime at which the TE device will be operated and other aspects must also be considered, such as the cost of materials, their toxicity and availability. For many applications, large scale installations will be essential for harnessing the full potential of thermoelectricity and the use of less efficient but cheap compounds might offer a valuable solution.

In this respect, Fe₂VAI has electronic properties potentially interesting for TE applications ($ZT\sim 0.13$ at 300K for Fe₂VAI_{0.9}Ge_{0.1} [1] and $ZT\sim 0.15$ at 300K for Fe₂VAI_{0.9}Si_{0.07}Sb_{0.03} [2]). Fe₂VAI has a L2₁ Heusler structure. It is more than a decade since Nishino *et al.* have reported its unusual properties, but the ground state of the intrinsic system is still unclear [3]. Fe₂VAI shows a semiconducting or semimetallic behaviour with a pseudogap of $\sim 0.1-0.27$ eV [4, 5]. Fe₂VAI is nonmagnetic (no long range FM order) but possesses magnetic anti-site defects and superparamagnetic clusters [6, 7]. It has a large specific heat at low T and first it was suggested to be a possible candidate for a 3d heavy-fermion system [3, 8]. Later, field-dependent specific heat measurements showed that the large specific heat was not an intrinsic behaviour and it was assigned to magnetic defects [9]. Fe₂VAI has also a negative resistivity slope at high T [8]. It has a dominant p-type transport character, with a high hole concentration of $n_h=4.8\times 10^{20}$ cm⁻³ [10] and shows a very large residual resistivity [3]. All these properties suggest that defects and disorder play an important role in this material.

Previous electronic structure calculations on Fe₂VAI were based on density functional theory (DFT) using usual exchange-correlations functionals such as the

generalized gradient and local density approximations (GGA, LDA) and predicted Fe₂VAI to be a compensated semimetal with a deep pseudogap of $\sim 0.1-0.2$ eV [11–13]. The presence of pseudogap with a finite density of states at the Fermi level is supported by optical reflectivity [5] and NMR [4] experiments, but the compensated character of carriers is in contradiction with Hall measurements [10] which found excess of holes. Usual DFT functionals are known to underestimate semiconductor band gaps and usually fail to describe strongly correlated systems. Hybrid functionals often allow to circumvent these problems and so constitute a promising alternative to better characterize Fe₂VAI.

In this letter we report the electronic and transport properties of Fe₂VAI using both the usual GGA functional of Perdew, Burke, and Ernzerhof (PBE [14]) and the recently developed B1-WC hybrid functional [15], which mixes the GGA of Wu and Cohen [16] with 16% of exact exchange. Whereas PBE reproduces the semimetallic character found in previous calculations, we predict Fe₂VAI to be a narrow gap semiconductor within B1-WC. Going beyond previous studies, we also investigate the role of single antisite defects and disorder on the transport properties. Our calculations strongly support that Fe₂VAI is intrinsically a semiconductor and that its semimetallic character originates from antisite defects and disorder, which introduce localized ingap and resonant states in the vicinity of the band gap. We show that such states negatively affect the power factor $PF=S^2\sigma$.

The calculations [17] were performed using the augmented plane wave and local orbital (APW+lo) method as implemented in WIEN2k [18]. We use the experimental lattice constant of 5.76 Å for a better comparison with previous calculations. The spin-orbit interactions and scalar relativistic effects were included. For the antisite defects and disordered configuration we considered supercells (SCs) with rhombohedral symmetry having 32 formula units (f.u) of Fe₂VAI which were derived from a 2x2x2 fcc cell with 4 atoms/cell along [1,1,1] direction [17]. The transport calculations were performed using Boltzmann transport formalism within the constant relaxation time approximation using BoltzTraP [19].

First, we consider the electronic properties. Our calculations describe Fe₂VAI to be nonmagnetic within both PBE and B1-WC. Although, it is described as a

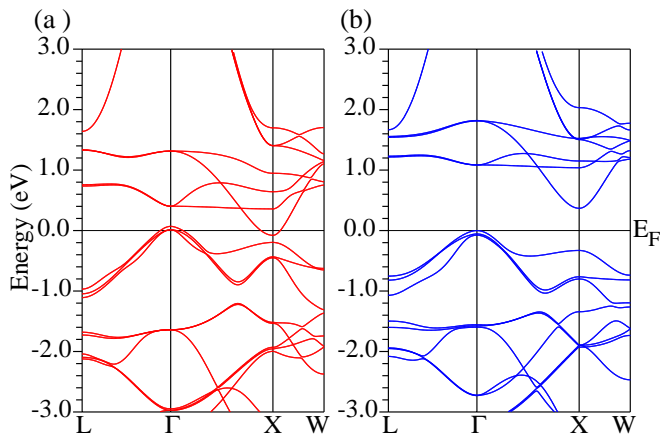


FIG. 1: (Color online) Electronic band structure of fcc Fe₂VAI within: (a)PBE and (b)B1-WC.

semimetal within PBE (Fig. 1a), as consistently obtained in previous calculations, it is predicted to be a semiconductor with an indirect band gap $E_g=0.34$ eV (Fig. 1b), within B1-WC. This is not specific to B1-WC: other hybrid functionals, such as B3PW91, similarly predict a semiconducting character, although the exact value of the gap depends on the percentage of exact exchange included in the functional. In comparison to PBE, B1-WC opens an indirect band gap by shifting up in energy the lowest conduction band (CB) states with mixed V and Fe e_g character with respect to the top valence band states with Fe t_{2g} character. The states close to CB minimum (X point in Brillouin zone) have a highly dispersive V e_g character, a very desired feature for good TE performance. We notice also that the charge of Al resulting from Bader analysis is equal to $1.68 |e|$. This highlights that Al p states hybridize with V and Fe d states and that Al does not donate all its 3 electrons to the Fe-V network, as sometimes assumed [11].

Let us now focus on the transport properties, using the constant relaxation time approximation. Within this approximation, S is independent of the relaxation time τ , whereas σ and the power factor $PF=S^2\sigma$ depend linearly on τ . Mainly due to Al deficiency [20], Fe₂VAI naturally forms as a hole-doped system with a carrier concentration $n_h=4.8\times 10^{20}$ cm⁻³. The value of τ was estimated at this carrier concentration by fitting the electrical resistivity ρ at 300 K to the experimental value of 0.75 m Ω cm [1, 21]. This yielded a hole relaxation time $\tau_h^{PBE}=0.9\times 10^{-14}$ s within PBE and $\tau_h^{B1-WC}=1.4\times 10^{-14}$ s within B1-WC. The electronic specific heat was also estimated for this hole-doped system. We obtained a value of 1.00 mJ/molK² within B1-WC, in better agreement with the experimental estimate of 1.5 ± 0.3 mJ/molK² [9] than the PBE value of 0.76 mJ/molK².

Electron doping of Fe₂VAI can be achieved from atomic substitution at Al site. We so estimated τ_e for electron doped Fe₂VAI_{1-x}M_x (M=Si, Ge) systems by fitting ρ at 300K to the experimental value of 0.65 m Ω cm corresponding to a doping $x = 0.03$ [1, 21]. Assuming that

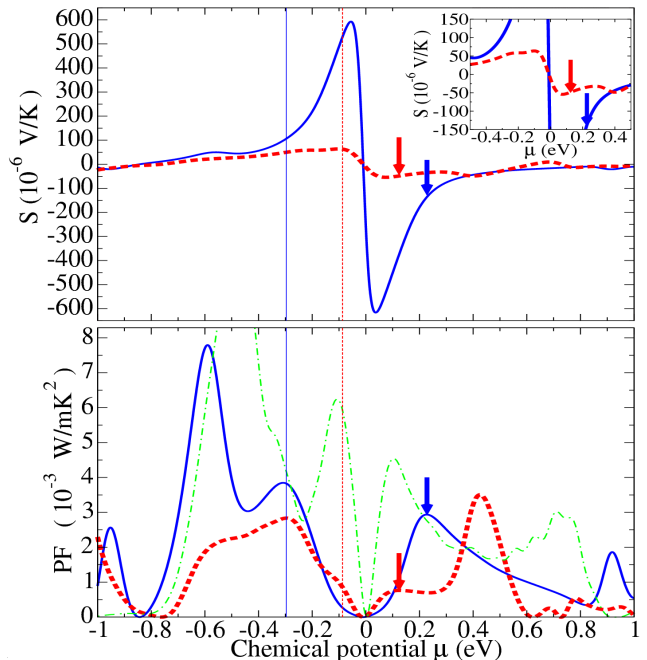


FIG. 2: (Color online) Thermopower S (S_{xx}) and power factor $PF=S^2\sigma$ (PF_{xx}) as a function of chemical potential μ of fcc Fe₂VAI within B1-WC(continuous) and PBE(dashed) at 300 K using τ_e^{B1-WC} and τ_e^{PBE} , respectively. μ corresponding to $n_h=4.8\times 10^{20}$ cm⁻³ are indicated by vertical lines. The maximum PF and corresponding S for n-type doping are indicated by arrows. PF of Bi₂Te₃ within PBE using $\tau_e=2.2\times 10^{-14}$ s is included for comparison (dot-dashed).

each atom M brings one additional electron, this corresponds to an electron concentration $n_e\sim 6.0\times 10^{20}$ cm⁻³, which adds to the initial n_h , assumed to be unchanged. Taking this into account, we get the electron relaxation times $\tau_e^{PBE}=1.5\times 10^{-14}$ s and $\tau_e^{B1-WC}=3.4\times 10^{-14}$ s. These values are slightly larger than those of the naturally formed hole-doped system, in qualitative agreement with the observation that the residual resistivity of Fe₂VAI decreases with doping at Al site [1, 21].

In Figure 2, we report the thermopower S and power factor PF of electron-doped Fe₂VAI along the x-axis ($S=S_{xx}$, $PF=PF_{xx}$) as a function of the chemical potential μ . The amplitudes of S and PF corresponding to μ for which the n-type PF reaches its maximum value are indicated by arrows. This is obtained for $\mu=0.23$ (resp. 0.12) within B1-WC (resp. PBE) and corresponds to a doping concentration $x = 0.03$ (resp. 0.05) for n-type Fe₂VAI_{1-x}M_x systems. Since we do not know the Al deficiency of these systems, we compare our values with the experimental values for which the maximum PF were achieved ($S\sim -120$:-130 μ V/K and $PF\sim 4$ -6 mW/mK² at 300 K [1, 21]). Within PBE, Fe₂VAI has a semimetallic character and S reaches a maximum value of ~ -55 μ V/K while PF saturates around ~ 0.7 mW/mK² for accessible x values. These values remain similar within a wide range of μ and cannot explain the much larger values reported experimentally. In contrast, within B1-

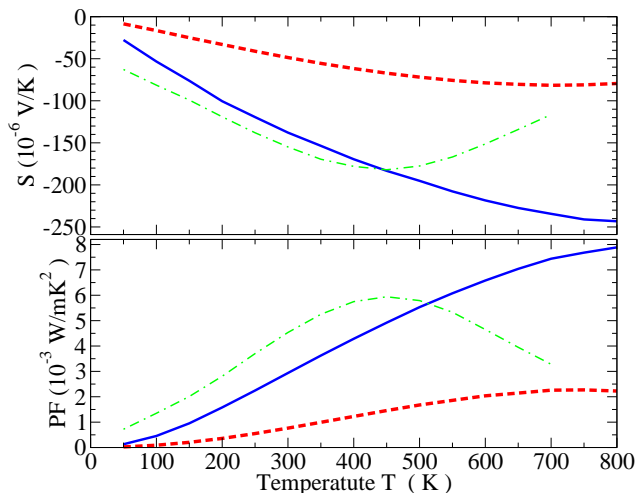


FIG. 3: (Color online) Temperature dependence of S_{xx} and PF_{xx} of fcc Fe_2VAI within B1-WC (continuous) and PBE (dashed) at x values of 0.03 and 0.05, respectively. Bi_2Te_3 values within PBE are also included (dot-dashed).

WC which describes Fe_2VAI as a semiconductor, we get larger values $S \sim -137 \mu V/K$ and $PF \sim 3 mW/mK^2$ in close agreement with experimental data. This demonstrates that a better description of Fe_2VAI is obtained when properly accounting for its semiconductor nature as obtained within B1-WC.

In Figure 3, we also report the temperature dependence of S and PF at fixed concentrations, corresponding to μ for which the n-type PF reaches its maximum value within B1-WC and PBE at 300K (see Fig 2). It can be seen that the theoretical S and PF do not saturate even up to 800 K within B1-WC. This shows the very good potential of Fe_2VAI for TE performance at high temperatures ($E_g=0.34$ eV) in comparison with other thermoelectric materials like Bi_2Te_3 (experimental $E_g=0.15$ eV). This contrasts however with the experimental observations, showing that S and PF are saturating around 200-250 K. We infer that this deterioration of the TE performance comes from defects and disorder, which change the electronic properties near the band gap.

In order to further prove this, we considered large SCs including 32 f.u. and performed B1-WC calculations including different types of single antisite defects and even considering a fully disordered configuration. Although the SC size corresponds to defect concentrations of ~ 0.03 , typically one-order of magnitude larger than what is observed experimentally [9], it is sufficient to treat the defects as isolated and to highlight their influence on the electronic and transport properties.

As illustrated in Fig. 4a, the V_{Fe} antisite defect, arising from the permutation of one V atom with Fe, reduces the band gap of Fe_2VAI to ~ 0.18 eV, by introducing localized d states into the gap, directly associated to the V and Fe atoms forming the defect. Moreover, this defect is magnetic with a magnetic moment of $4\mu_B/\text{defect}$ localized on the defect, a value which agrees well with that of $3.7\mu_B/\text{defect}$ found in specific heat and NMR ex-

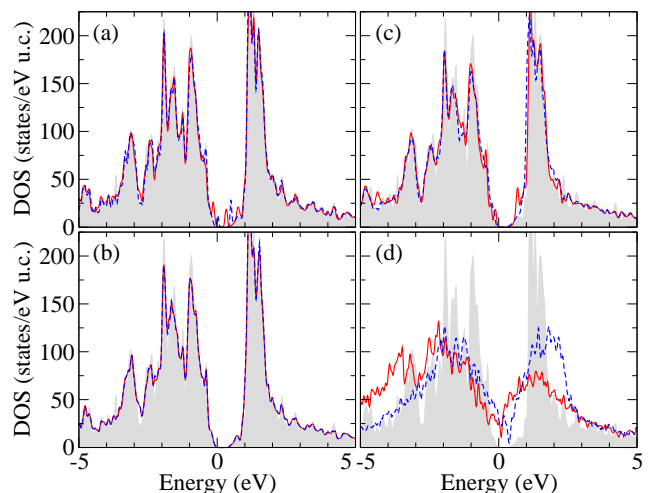


FIG. 4: (Color online) Spin up (continuous) and down (dashed) total density of states (DOS) for: (a) V_{Fe} , (b) V_{Al} , (c) Fe_{Al} antisite single defects, and (d) disordered configuration. The DOS of intrinsic Fe_2VAI is shown as a gray background.

periments [7, 9]. By contrast, the V_{Al} antisite defect is non-magnetic and does not introduce any ingap state (Fig. 4b). Finally, the Fe_{Al} antisite defect introduces resonant Fe d states at the bottom (resp. top) of conduction (resp. valence) bands (Fig. 4c). Again, this defect is magnetic with a magnetic moment of $4.6\mu_B/\text{defect}$. So, our B1-WC calculations reveal that some antisite defects are magnetic and that only those introduce localized ingap states and resonant states close to the gap region, significantly changing the electronic properties of Fe_2VAI .

In order to model further the effect of site disorder, we also considered a disordered configuration, arising from an arbitrary occupancy of the different sites within the SC and including 20 antisite defects (8 V_{Fe} , 6 V_{Al} , and 6 Fe_{Al}). The change in the electronic properties close to the gap region is even more obvious for this disordered configuration for which a semimetallic behaviour with a pseudogap and a magnetic moment of $53.5\mu_B/\text{cell}$ is obtained (see Fig. 4d). These results clearly establish that the semimetallic character seen in experiments can be explained from antisite defects and disorder.

It is now very interesting to explore the effect of the localized ingap and resonant d states on the transport properties. Mahan and Sofo have shown that a narrow energy (delta-shape) distribution of the electronic states participating in the electronic transport is needed in order to maximize ZT [22]. Therefore, such localized ingap and resonant d states are expected to increase PF in the cases where these states have a significant weight with respect to the background states [22]. However, as summarized in Fig. 5, our transport calculations including antisite defects and disorder show that the localized ingap d states do not increase PF , which takes smaller or comparable values for accessible n_e doping values. For defect concentration seen in experiment, the reduction should be less apparent but these calculations establish that antisite defects will never boost the TE performance.

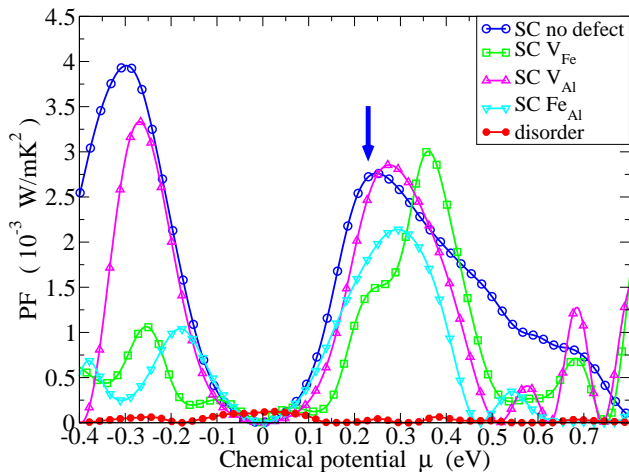


FIG. 5: (Color online) PF_{xx} as a function of μ for the antisite defects and disordered configuration of Fe_2VAl within B1-WC at 300 K using τ_e^{B1-WC} . x value of 0.03 for the intrinsic Fe_2VAl is indicated by arrow. Note that for defects and disorder, this x value is achieved at smaller μ .

For n_e value corresponding to the maximum PF of intrinsic Fe_2VAl ($x=0.03$), we show the temperature dependence of S and PF in Figure 6. The antisite defects and disorder have a detrimental effect on PF, decreasing and saturating its values with T . For V_{Fe} defect, S and PF values are saturating at ~ 350 K, behaviour seen in experiment. It is interesting to note that our disordered configuration have a "hole-like" dominated S , even at $x=0.03$. This suggests that the p-type character of Fe_2VAl may originate also partly from site disorder, and not only from off-stoichiometry of the constituents.

In summary, our B1-WC calculations show that Fe_2VAl is an indirect narrow band gap semiconductor

with a highly-dispersive $V e_g$ CB and three fold degen-

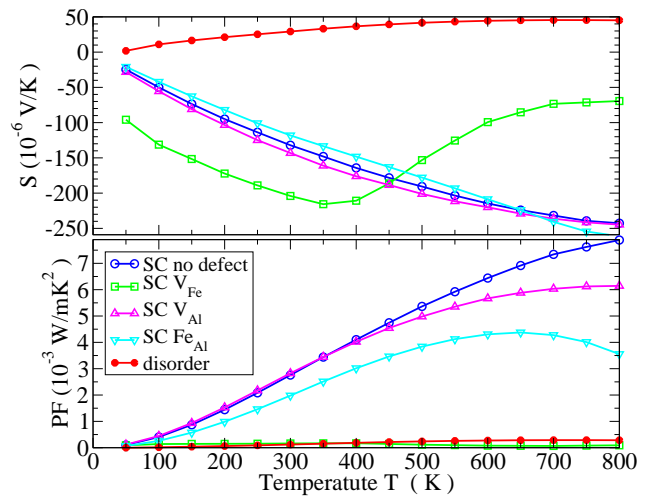


FIG. 6: (Color online) Temperature dependence of S_{xx} and PF_{xx} for the antisite defects and disordered configuration of Fe_2VAl within B1-WC at x value of 0.03.

erate CB minimum, all features highly-compatible with good intrinsic TE performances. Our calculations including anti-site defects also demonstrate that the semimetallic character of Fe_2VAl seen in experiments can be explained from atomic disorder. Some anti-site defects are magnetic and introduce localized ingap and resonant states in the gap region. These defects tend to decrease the good intrinsic TE performances of Fe_2VAl .

Acknowledgments

We acknowledge financial support from Walloon Region through the CoGeTher, EnergyWall project.

-
- [1] Y. Nishino, S. Deguchi, and U. Mizutani, *Phys. Rev. B* **74**, 115115 (2006).
- [2] M. Mikami, S. Tanaka, and K. Kobayashi, *J. Alloys Comp.* **484**, 444 (2009).
- [3] Y. Nishino *et al.*, *Phys. Rev. Lett.* **79**, 1909 (1997).
- [4] C. S. Lue and J. H. Ross, Jr., *Phys. Rev. B* **58**, 9763 (1998).
- [5] H. Okamura *et al.*, *Phys. Rev. Lett.* **84**, 3674 (2000).
- [6] M. Vasundhara, V. Srinivas, and V. V. Rao, *Phys. Rev. B* **78**, 064401 (2008).
- [7] C. S. Lue *et al.*, *J. Phys.: Condens. Matter* **13**, 1585 (2001).
- [8] Y. Nishino, *Intermetallics* **8**, 1233 (2000).
- [9] C. S. Lue *et al.*, *Phys. Rev. B* **60**, R13941 (1999).
- [10] M. Kato *et al.*, *J. Jpn. Inst. Met.* **62**, 669 (1998).
- [11] R. Weht and W. E. Pickett, *Phys. Rev. B* **58**, 6855 (1998).
- [12] D. J. Singh and I. I. Mazin, *Phys. Rev. B* **57**, 14352 (1998).
- [13] G. Y. Guo, G. A. Botton, and Y. Nishino, *J Phys.: Condens. Matter* **10**, L119 (1998).
- [14] J. P. Perdew, K. Burke, and M. Ernzerhof, *Phys. Rev. Lett.* **77**, 3865 (1996).
- [15] D. I. Bilc, R. Orlando, R. Shaltaf, G.-M. Rignanese, J. Iniguez, and Ph. Ghosez, *Phys. Rev. B* **77**, 165107 (2008).
- [16] Z. Wu and R. E. Cohen, *Phys. Rev. B* **73**, 235116 (2006).
- [17] See EPAPS Document No. ... for technical details of the calculations.
- [18] P. Blaha *et al.*, WIEN2K, An Augmented Plane Wave + Local Orbitals Program for Calculating Crystal Properties, Techn. Universitat Wien, Austria, 2001.
- [19] G. K.H. Madsen and D. J. Singh, *Comp. Phys. Comm.* **175**, 67 (2006).
- [20] I. Maksimov *et al.*, *J Phys.: Condens. Matter* **13**, 5487 (2001).
- [21] M. Vasundhara, V. Srinivas, and V. V. Rao, *Phys. Rev. B* **77**, 224415 (2008).
- [22] G. D. Mahan and J. O. Sofo, *Proc. Nat. Acad. Sci.* **93**, 7436 (1996).